Department of Geology
Utah State University
Logan, UT 84322-0705
U.S.A.

SPATIAL AND TEMPORAL ANALYSIS OF 1200 LANDSLIDES IN A 900km² AREA, MIDDLE ROCKY MOUNTAINS,

WYOMING, U.S.A.

JAMES McCALPIN, JOHN B. RICE, Jr.
Department of Geology, Utah State University, U.S.A.

SYNOPSIS An inventory of approximately 1200 landslides in a 900 km^2 area in the Salt River Range, western Wyoming, U.S.A., reveals regional and temporal controls on the landsliding process. Sliding is strongly controlled by eight weak formations in the 21 stratigraphic units of Cambrian through Cretaceous age. Morphologic dating of slides suggests that rockslides, slump-flows, and debris flows have occurred rather uniformly in time within the Holocene. In contrast, earthflows seem to be triggered more by cool/wet climatic epicycles in the last 5,000 years.

INTRODUCTION

The authors performed a landslide inventory of 900 km^2 under contract to the U.S. Forest Service in 1985. We soon realized that the large number (roughly 1200) of mapped slides contained valuable information on spatial and temporal controls of landsliding. The contract specified that each landslide be classified by type following a modification of Varnes (1978) classification. However, no classification of age or activity was required, mainly because no universally-accepted system existed. The senior author had proposed a morphologic-based landslide age classification system for use in inventory studies in 1984 (McCalpin, 1984), so this system was used to roughly "date" each mapped slide. To validate whether this system was truly reliable, independent age data were gathered from a small sample of particular landslide types (rockslides and rockfall avalanches). The validated age classification scheme, plus correlation of landslides with mapped geologic units, form the basis for a regional assessment of spatial and temporal distribution of landslides during Holocene time in an undeveloped region of the Rocky Mountains, U.S.A. In particular, we test the hypothesis that most currently inactive landslides originated during cooler/wetter glacial episodes.

STUDY AREA

The inventory area comprises 900 km^2 in the Salt River Range of western Wyoming (Fig. 1). The Salt River Range is a 120 km-long, 25 km-wide north-south trending range of mountains rising to an average crest elevation of 3200 m. The Range is bounded on the west by the Grand Valley Fault (a Neogene normal fault) and Star Valley (elev. 1900 m), and on the east by the Greys River. The geology of the Salt River Range is dominated by the west-dipping Absaroka Thrust fault, which crops out on the eastern side of the range (Rubey, 1973 Fig. 2). The majority of the range is composed of massive Paleozoic carbonates (maximum stratigraphic thickness 1975 m) and Triassic-Jurassic carbonate and clastic units (totalling 2150 m stratigraphic thickness) which form the upper plate of the Absaroka Thrust. These two lithologic packages are tightly folded into synclines and anticlines which generally parallel the north-south trend of the range. Beneath the thrust on the eastern side of the range,

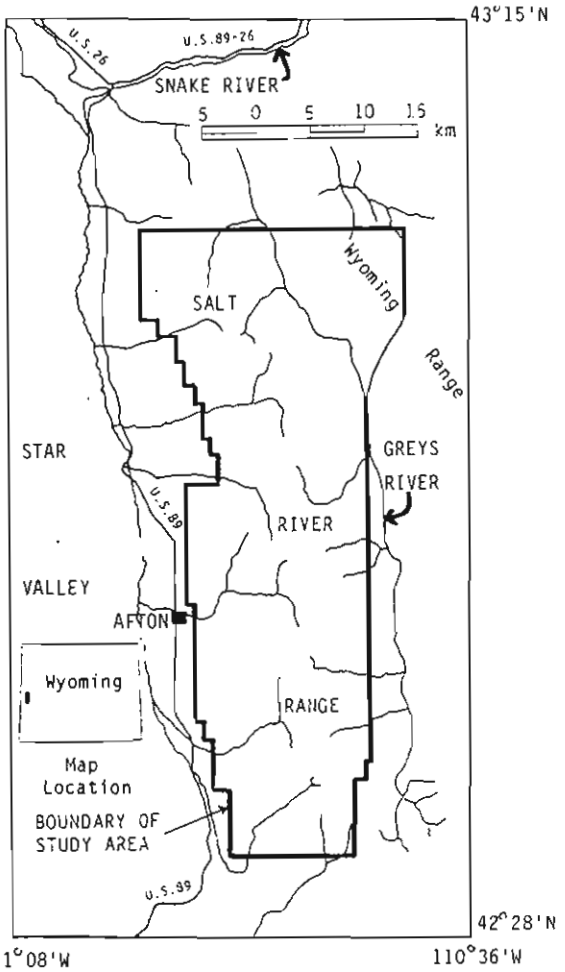

Fig. 1. Location of the study area. Landslides were inventoried over a 900 km^2 irregular area centered on the Salt River Range crest.

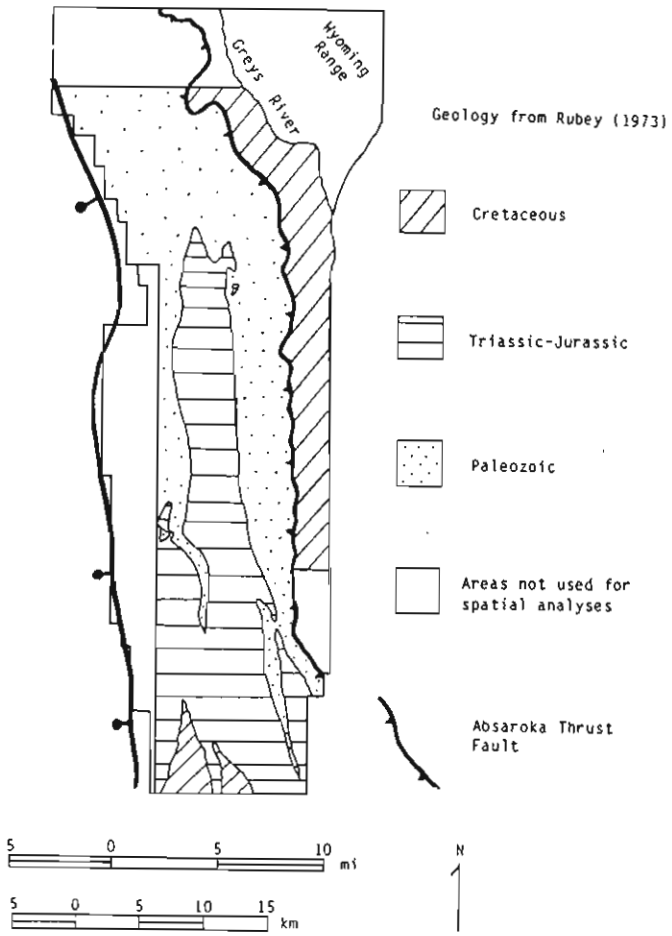

Fig. 2. Simplified geologic map of the landslide inventory area, Salt River Range, Wyoming. The range crest generally lies immediately west of the Absaroka Thrust, where highest peaks are underlain by massive Paleozoic carbonate units. West-flowing drainages (Fig. 1) therefore cross Paleozoic and Triassic-Jurassic strata, broadly folded, of the upper thrust plate. East-flowing valleys head in the high Paleozoic peaks, but soon cross the thrust and are developed in Cretaceous clastics of the lower thrust plate.

lower plate rocks of Cretaceous age (siltstone, shale, minor sandstone) are highly deformed and dip at various angles. These three stratigraphic packages differ in their susceptibility to landsliding, as explained further.

INVESTIGATION PROCEDURE

Landslide Inventory

Landslides of all types and ages were identified and delineated on 1:15,840 scale color aerial photographs. Slides were classified into one of four major type categories, following a modification of Varnes (1978) classification (Fig. 3). We found that

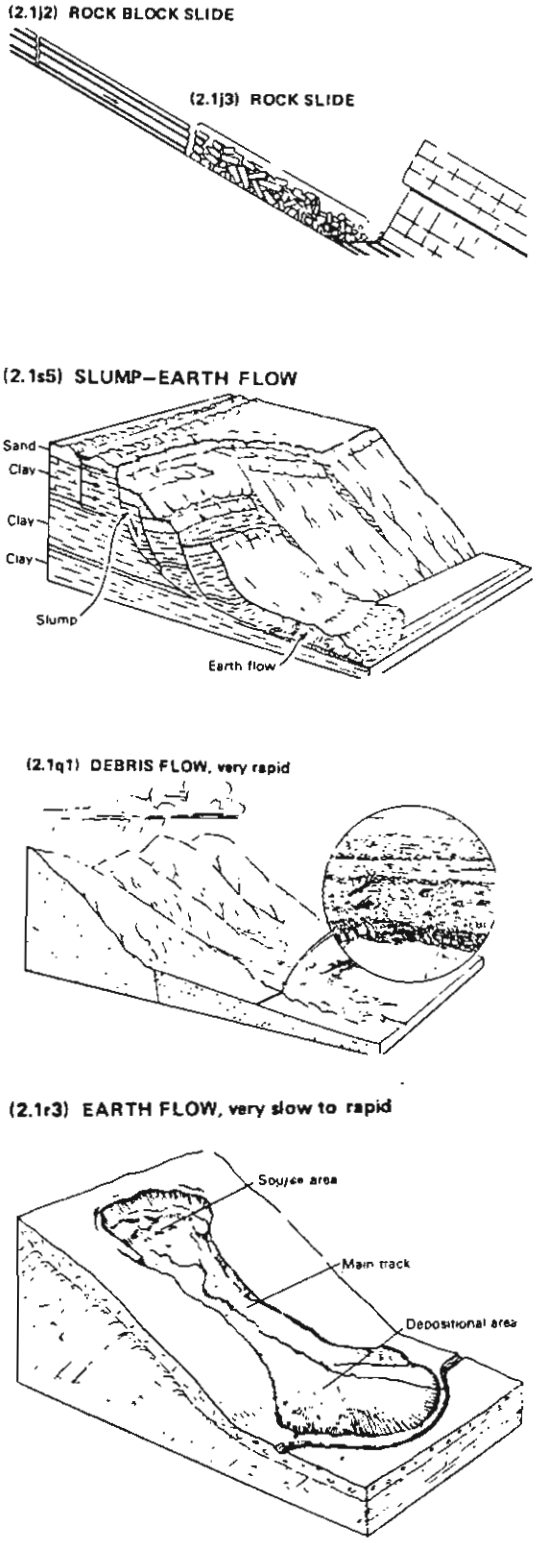

Fig. 3. Diagrammatic sketches of the dominant types of mass movements in the Salt River Range. Classification scheme and block diagrams are from Varnes (1978).

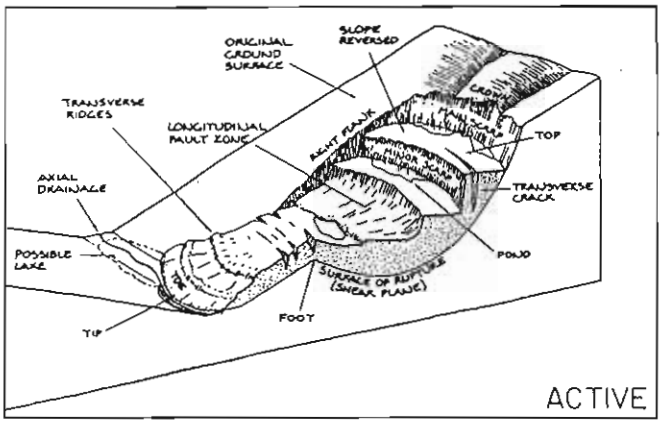

Fig. 4. Diagrams showing the morphologic age classification for a typical slump-flow landslide. From McCalpin, 1984.
a. Active (class 1). At the head scarp features are sharp and unvegetated, backs of rotated blocks pond local drainage. Nearer the toe open transverse and radial cracks occur associated with lateral spreading and overthrusting of turf. Toe may dam the drainage.

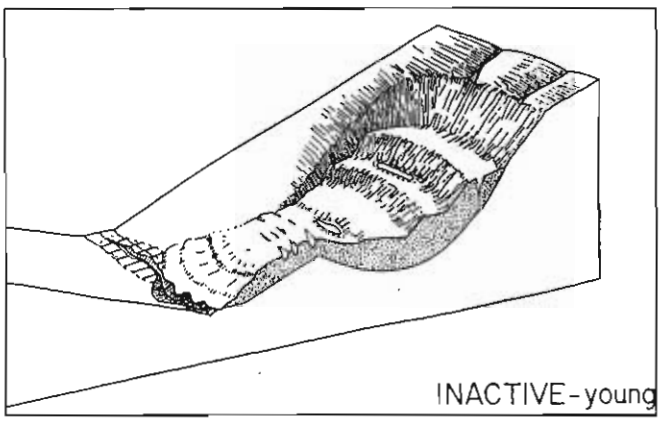

b. Inactive-young (class 2). Headscarp and internal scarps become rounded and vegetated, local ponds fill with sediment. open cracks fill with debris. Toe ridges are subdued. Axial drainage breaches the toe dam and drains the natural lake.

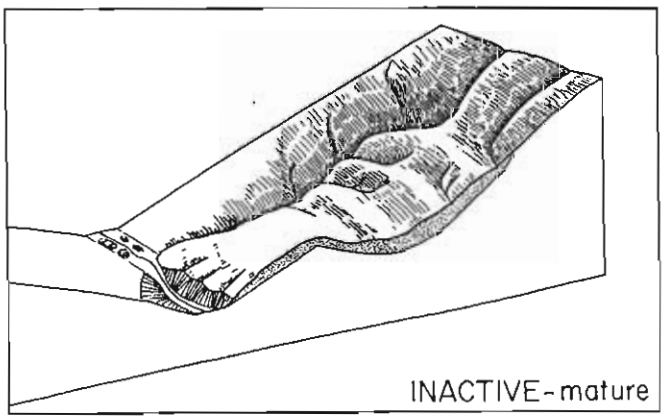

c. Inactive-mature (class 3). Head scarp and internal scarps are dissected by local drainages, which advance headward along scarp margins. Deposition obscures initial sediment traps, and vegetation invades from off the slide. Toe is eroded back by stream meandering.

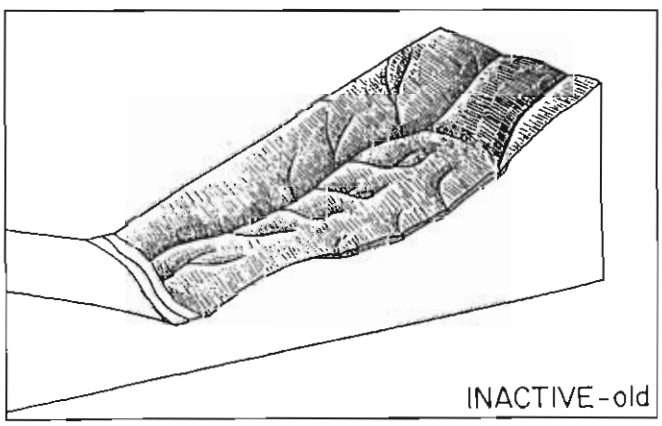

d. Inactive-old (class 4). Fluvial drainage completely dissects and obscures the slide mass. The only hints of past sliding are anomalously curved drainages below a steepening in the hill gradient, and perhaps small displacement of the axial drainage.

a more detailed type classification was not feasible because almost all slides displayed characteristics of more than one slide type, e.g. they were composed of both soil and rock, and exhibited both slump and flow behavior in varying degrees. Slides were classified by age into one of four major categories based on morphologic modification (Fig. 4). This approach works best for single-event slope failures which move and then become stabilized, rather than for slowly creeping slides or flows. However (as discussed later) flows only constitute 18% of landslides. Due to a lack of roads in the study area access was limited, and only about 2% of the 1200 slides were checked in one field. On those that were checked sampling was limited to age-diagnostic parameters, as discussed below.

Relative Dating

Because the morphologic age classification was only crudely calibrated to an absolute age scale (McCalpin, 1984), more calibration data were needed. It was not anticipated that radiocarbon-datable samples could be obtained from a significant number of slides, so emphasis was placed instead on relative dating. The relative dating (RD) method is extensively used in dating glacial and periglacial deposits (Burke and Birkeland, 1979). Moraines and rock glaciers of Pinedale and Neoglacial age (Porter and others, 1983) were present in the Salt River Range in close proximity to landslides. Not only could cross-cutting relations between moraines and landslides give a clue to slide age, but a statistical comparison of RD parameters could determine whether landslides were older than, contemporaneous with, or younger than moraines and rock glaciers. To test these hypotheses, standard RD parameters (Appendix A) were collected from 21 rockslides and 19 glacial/periglacial deposits. Rockslides were used for the comparison because: 1) they are texturally similar to bouldery glacial deposits, and 2) they result from single, brief depositional events without periodic reactivation.

SPATIAL ANALYSIS

Frequency of Landslide Types

Of the 1173 landslides mapped, 76% were slump-flows, 16% were debris flows, 6% were rockslides, and 2% were earthflows (Table 1a). However, the relative

TABLE 1a

Landslide Type	Landslide Age 1	1+2	2	2+3	3	3+	3+4	4	Total
Slump-earth flow	59	2	292	52	364	3	3	117	892
Debris flow	25	35	82	10	23	-	-	7	182
Rockslide	6	-	23	-	25	6	-	15	75
Earth flow	3	-	18	-	3	-	-	-	24
Totals	93	37	415	62	415	9	3	139	1173
% in 4 Age-Classes	9	-	40	-	39	-	-	12	-

TABLE 1b

Paleozoic Section:

Landslide Type	Landslide Age 1	1+2	2	2+3	3	3+	4	Total
Rockslide	3	-	9	-	14	3	3	32
Slump-earth flow	7	-	30	-	52	1	28	117
Debris flow	17	26	26	3	1	-	-	73
Total	27	26	65	3	67	3	31	222
% in 4 Age-Classes	18	-	36	-	32	-	14	-

TABLE 1c

Triassic-Jurassic Section:

Landslide Type	Landslide Age 1	1+2	2	2+3	3	3+	4	Total
Rockslide	1	-	8	-	16	3	7	25
Slump-earth flow	12	-	37	2	89	2	40	182
Debris flow	8	11	33	3	13	-	-	68
Total	21	11	78	5	108	5	47	275
% in 4 Age Classes	10	-	31	-	42	-	17	-

TABLE 1d

Cretaceous Section:

Landslide Type	Landslide Age 1	1+2	2	2+3	3	3+4	4	Total
Slump-earth flow	16	-	82	36	83	3	10	230
Earth flow	1	-	10	-	2	-	-	13
Total	17	-	92	36	85	3	10	243
% in 4 Age Classes	7	-	45	-	44	-	4	-

percentages were different in each of the three lithologic packages defined previously. In the Paleozoic section (Table 1b) (dominated by massive, steeply-dipping carbonates), of 222 slides inventoried 53% were slump-flows, 33% were debris flows, and 14% were rockslides. Rockslides were relatively more abundant in this lithology due to favorable geometries for bedding-plane translational slides of massive resistant carbonates lying on weaker shales and mixed clastic units. Debris flows were also relatively abundant, forming from debris slides in colluvium derived from nonresistant clastic units interbedded with the carbonates.

Slides in the Triassic-Jurassic section (Table 1c, 275 inventoried) were composed of 66% slump-flows, 25% debris flows, and 9% rockslides. The decrease in rockslides and increase in slump-flows compared to the Paleozoic section reflects more weak, fine-grained clastic units and fewer resistant sandstones and carbonates in this lithologic package. The Cretaceous section (Table 1d), in contrast with the other two lithologic packages, is dominated by more fluid flows and slump flows. Of 243 slides inventoried, 95% were slump-flows, 5% were earthflows (not present in the

other packages) and there were no rockslides. This distribution reflects the weak, semi-consolidated nature of units within the Cretaceous section, which are prone to retrogressive rotational slumping with extensive flow mobilization of slide toes.

Landslide Densities

The percent of the total outcrop area of each of the three lithologic packages involved in landsliding differs considerably between rock types. In the Paleozoic section landslides cover an average of 15% of outcrop area, varying from 28% in the northern part to only 8% in the southern part of the mapped area. Roughly 10% of the Triassic-Jurassic section outcrop area is involved in sliding. In contrast, landslides cover 73% of the outcrop area of Cretaceous rocks, ranging from a high of 90-95% cover in the north, to about 50% in the south. Such high percentages of landslide cover make bedrock mapping difficult in these poorly-indurated Cretaceous rocks and assignment of slides to individual formations isgenerally not possible.

Stratigraphic Units Prone to Landsliding

Fig. 5 shows the density of landslides (slides/km^2) that occur within each formation in the

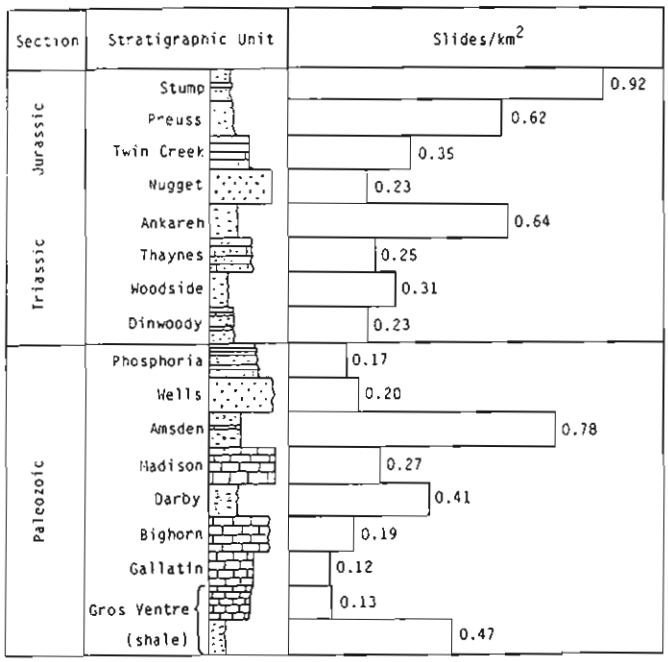

Fig. 5. Landslide densities within each stratigraphic unit in the pre-Cretaceous section. Only age classes 1 and 2 were counted; older slides are harder to detect and numbers may not be representative.

Paleozoic and Triassic-Jurassic lithologic packages. Units with the highest slide densities (Gros Ventre shale, Darby Formation, Amsden Formation in the Paleozoic section; Woodside, Ankareh, and Stump Formations in the Triassic-Jurassic section) are invariably fine-grained clastic units, with minor interbedded siltstones, sandstone, conglomerates, and breccias. Adjacent resistant strata (massive carbonates and sandstones) are often undermined by failures in the weaker units, leading to massive rockslides. Because strata may be either in normal or overturned stratigraphic order, failures in a given weak unit (e.g. Amsden Fm.) lead to failures in the upslope resistant unit, which may be stratigraphically higher (Wells Fm.) or lower (Madison Fm.).

Correlation with Topography

It was initially anticipated that landsliding would be heavily influenced by glacially over-steepened valley walls, resulting in a good correspondence between glaciated valley segments and landsliding. This association does occur in the Cretaceous section on the east side of the Salt River Range. Here valley glaciers originating in the high country underlain by Paleozoic rocks descended down across the Absaroka Fault. Soft Cretaceous rocks were severely scoured into U-shaped valleys for a distance of 4 - 6 km. After ice retreat, the unsupported oversteepened valley walls began retrogressive slump-flow failure, which in some cases has completely dissected the 1.5-2.0 km wide interfluves which originally separated the U-shaped valleys.

In the more resistant Paleozoic and Triasic-Jurassic sections, the relation of landsliding and glaciation is less clear. Many slumps and rockslides do occur where dipping strata have been undercut by glacial valley erosion. However, slides are nearly as abundant downvalley of the glacial limits. This is particularly true on the western side of the range, where the lower, unglaciated reaches of valleys are steep, V-shaped canyons which lead down to the range fault. Continuing Quaternary uplift along the Grand Valley Fault (Piety, 1987) has led to constant stream incision and valley wall steepening, which in turn has triggered landslides in steeply-dipping strata via undercutting. Age data (discussed in the next section) confirm that these slides are not merely post-glacial, but have been occurring more or less continuously during the Holocene.

TEMPORAL ANALYSIS

During inventory mapping each landslide was assigned to one of four major age classes based on the degree of morphologic "freshness" exhibited by certain slide features. Where slides contained a mixture of younger and older-appearing features which were too small to map separately, two age designations were used (e.g. 2+3). A distinct group of rockslides which appeared to have fallen onto disintegrating glacial ice in the waning stages of deglaciation were separated into group 3+. Thus the original four major age groups were combined to include as many as eight age categories.

The absolute ages of each morphologic category were initially defined based on C-14 dates for landslides and glacial deposits elsewhere in the Rocky Mountains. For example, the slide at Devil's Elbow, Wyoming (slightly older than 4100 yr BP;Bailey, 1971) exhibits morphology intermediate between our age classes 2 and 3. Thus the class 2/3 boundary is tentatively placed at roughly 5000 yr BP, or at the transition from the dry, warm Altithermal period to the cooler, moister Neoglacial period (Denton and Porter, 1970). The older limit of class 3 was defined as the beginning of deglaciation, since in most cases it was easy to determine if slides pre- or post-dated glaciation in mountain valleys; this age is roughly 14,000 - 15,000 yr BP in the Rocky Mountains (Porter, 1980). Class 4 slides either predated or were contemporaneous with glaciation, as evidenced by cross-cutting relations with moraines, glacial valleys, or patterned ground. Class 1 (historic) slides must either displace cultural features (less

than 100 years old) or have documented historic movement.

Temporal Distribution from Photgeology

The first approximation for determining the chronology of landsliding is the apparent temporal distribution of the four major age classes. For 1173 slides, 9% were class 1 (0-100 yr BP), 40% were class 2 (100-5,000 yr BP), 39% were class 3 (5,000-14,000 yr BP) and 12% were class 4 (older than 14,000 yr BP). It is interesting to note that:1) classes 2 and 3 have similar numbers of slides, despite the fact that class 3 spans almost twice as much time as does class 2, and 2) despite the very short span of class 1 (100 yr, or less than 1% of post-glacial time) a surprising 10% of post-glacial slides fell into this age class. The number of landslides occurring per km^2 per 1000 yr can be calculated for post-glacial time (last 14,000 yrs) and yields : class 1, 1.24 slides/km^2/1000 yr; class 2, 0.11 slides/km^2/1000 yr; and class 3, 0.06 slides/km^2/1000 yr. Before making any conclusions about the frequency of landsliding in the past, however, two questions need to be addressed. First, is the morphologic age classification reliable, and are its' assumed absolute age ranges even approximately correct? Second, are the landslides mappable today all the landslides which have occurred, or have some been obscured by erosion or reactivation, as the decreasing frequency of slides with increasing age suggests? The first question will be answered by comparing weathering data from landslides of unknown age and from moraines of known age. The second question will be addressed by estimating the effect of obscuring mechanisms on each type of slide.

Relative-Dating of Rockslides and Glacial/Periglacial Deposits

RD data (parameters listed in Appendix A) were collected from eight Pinedale moraines, nine Holocene moraines, three rock glaciers and a protalus rampart. Comparison of these data with C-14-calibrated data from the nearby Wind River Mountains (Mahaney et al, 1984) suggested that six of the Holocene moraines represented an early Holocene advance (about 10,000 yr. B.P.), while the remainder of the moraines and rock glaciers were of Neoglacial age (0-5,000 yr. B.P.). Quantitative comparison of RD data from deposits of Pinedale, early Holocene, and Neoglacial age with data from rockslides of unknown age was performed using a multivariate statistical technique known as cluster analysis. The output of a cluster analysis is a hierarchical tree, or dendrogram, which shows the hierarchy of similarities among pairs of objects in the data set (Romesburg, 1984). Objects which occur on the same branch are most similar to each other. The farther to the right, or the closer to the main branch of the tree that branches connect, the more dissimilar the objects on those branches are.

A number of cluster analyses were run using the unweighted pair-group method using arithmetic averages (UPGMA) using the VAX 11780 computer at Utah State University and the programs CLUSTAR/CLUSTID written by Charles Romesburg and Kim Marshall. Dendrograms were constructed using five, six and eight RD parameters, for both rockslides alone and for rockslides and glacial deposits combined. Because some pairs of the original RD parameters were highly correlated it was necessary to delete some parameters lest the pairs unduly influence the cluster outcome. In the following section, only the results of the five-parameter dendrogram containing all stations will be discussed; the reader is referred to Rice (1987) for details of the other analyses, which produced dendrograms similar to the one described here.

Fig.6 shows the clustering of rockslide and moraine stations. The first-order cut of the tree

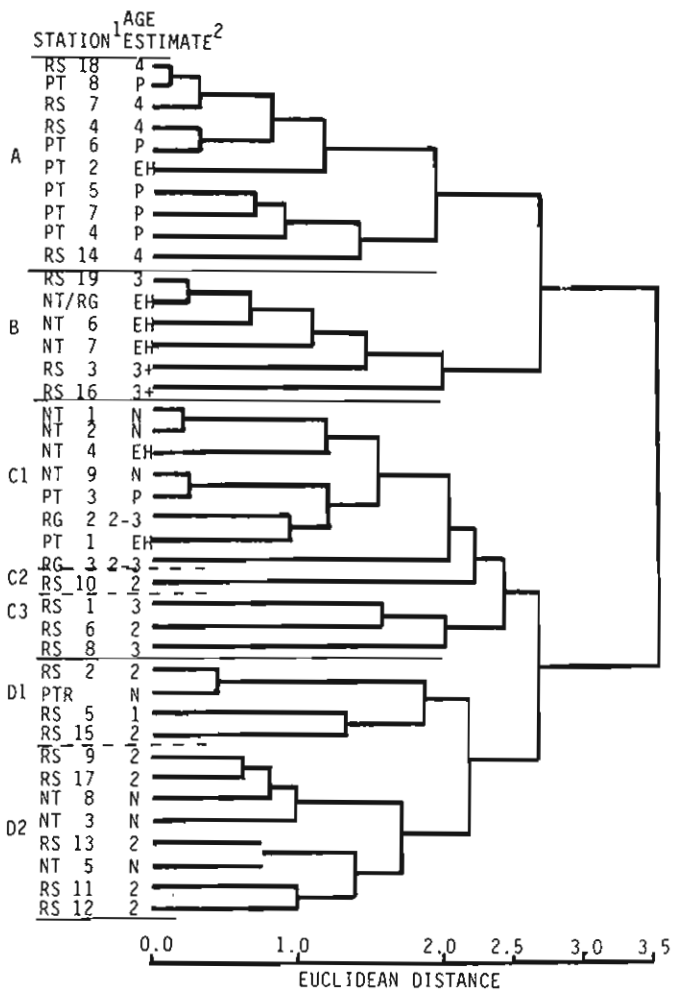

Fig. 6. Dendrogram of cluster analysis using all stations and 5 RD parameters. RD parameters-boulder pit depth, surface boulder frequency, ridge crest width, outer slope angle, soil profile development, Cophenetic Correlation Coefficient=0.624. [1]Station symbols: RS-rockslide; NT,PT- moraine; RG- rock glacier; PTR- protalus rampart. [2]Age symbols: 1,2,2-3, 3,3+,4- landslide age classes; N-Neoglacial; EH-early Holocene; P-Pinedale.

divides clusters A and B from clusters C and D. Notably, cluster A-B contains all the old rockslides (3+ and 4) plus all the Pinedale and most of the early Holocene moraines, while cluster C-D contains all the younger rockslides and moraines. A second-order cut at Euclidian distance 2.5 yields four clusters (A,B,C, and D). Each cluster contains both landslides and moraines, of various lithologies, scattered over a broad range of elevation. This range suggests that RD differences due to original morphology or variable weathering rates should not be important. Cluster A contains all the Pinedale stations but one, and all

the age class 4 rockslides, indicating it is the oldest cluster. Cluster B contains all the 3+ rockslides and a majority of the early Holocene moraines, suggesting it is slightly younger than cluster A. Cluster C is composed of a mixture of age class 2, 2-3, and 3 rockslides and Pinedale, early Holocene, and Neoglacial moraines, suggesting a younger age than clusters A or B, but with possible interference effects from variable lithologies or weathering rates. Cluster D contains nothing but class 1 and 2 rockslides and Neoglacial moraines, indicating it is the youngest cluster.

A third-order cut at Euclidean distance 2.1 yields a total of seven clusters, by dividing C into C1, C2, and C3, and D into D1 and D2. Our interpretation is that clusters at this level of subdivision are being dominated by non-age differences, due to variations in original deposit morphology and weathering rates. For example, cluster C1 contains all the glacial and periglacial deposits of cluster C, while clusters C2 and C3 contain all the rockslides: this suggests differences in initial morphology outweigh those due to age. In addition, although cluster C is thought to be older than cluster D, some parameters for C1 are actually less weathered than those same parameters in D, leading to ambiguity as to relative age. Likewise, a comparison of average RD parameter values between clusters D1 and D2 indicates that, for some parameters D1 appears older, but for others D2 appears older.

More evidence on the age-limitations of the cluster analysis comes from stations PT6 and PT7 in cluster A. These two stations were placed on the same moraine crest at locations 500 m apart. Although theoretically their RD values should have been identical, due to minor microclimatic and lithologic variations there were slight differences. These small "random" differences in RD values will eventually lead to their being split into different branches of the dendrogram. Clearly, this split does not have age significance, and any splits even further to the left (Euclidean distance of 1.9 or less) should not be construed as age indicative.

Therefore, the cluster analysis seems to have age significance at least to the four-cluster subdivision, which separates age class 4(cluster A), 3+ (cluster B), 3 (cluster C), and 2 (cluster D) rockslides. The fact that cluster C contains both age class 2 and 3 rockslides indicates that in some cases, especially where rockslides form and then are later reactivated by periglacial ice into rock glaciers (stations RG2 and RG3), the morphologic method may misclassify deposits. Overall, the cluster analysis supports the validity of the morphologic age classification, and lends confidence that the original absolute ages for classes are approximately correct.

Correcting the Apparent Temporal Distribution

We define the distribution of landslide ages today as the apparent temporal distribution. This apparent distribution is only identical to the actual temporal distribution if every landslide that has ever occurred in our study area is still visible and was mapped by us. Admittedly, it is possible that some small landslides (less than 30 m in diameter) were missed due to resolution limitations of the 1:15,480 aerial photographs. However, this limitation would apply to all age classes. There are three major processes which tend to obscure or eradicate traces of landslide activity. First, continuous erosional modification of landslides steadily obscures them. This is the basis for the morphologic age classification, but in the older age classes (3, 3+, 4) it is possible that some slides were so obscured as to be overlooked. Second, more recent landslide toes can bury older ones, thus hiding evidence of earlier movement. This is a common problem with debris flows, where generations of flow lobes have accumulated atop each other to build debris fans. As an example, 81% of all mapped debris flows were age class 1 or 2 deposits. Third, reactivation of older landslides rejuvenates the slide surface, leading to a younger age designation. If reactivation involves the entire pre-existing landslide, then all surface traces of older movement are often lost.

To correct the apparent temporal distribution for the effects of those three mechanisms, we have made subjective judgements as to how severely each mechanism has affected each type of slide through time. The percent detection values given in Table 2 are admittedly subjective, but are based on many man-months of photogeologic mapping and field checking of this particular mountain range. For post-glacial time, the apparent temporal distribution (Table 1) has been corrected using the assumption that only a certain percentage of the slides which originally occurred were detected by us. The corrected temporal distribution, which is identical to the actual temporal distribution if our detection values are accurate, is shown in Table 3 for each major type of landslide.

TABLE 2: PERCENT DETECTION ESTIMATES FOR LANDSLIDES

Slide Type	Age-Class 1	Age-Class 2	Age-Class 3	Age-Class 3+
Rockslides	100%	95% (A= 5%)	85% (A= 10%) (C= 5%)	75% (A= 15%) (C= 10%)
Slump-Earth flows	100%	80% (A= 5%) (C= 15%)	50% (A= 20%) (C= 30%)	
Debris flows	99% (B= 1%)	50% (A= 20%) (B= 30%)	10% (A= 40%) (B= 50%)	
Earth flows	100%	65% (A= 10%) (C= 25%)	25% (A= 25%) (C= 50%)	

A= % slides undetectable due to erosional modification

B= % slides obscured by younger deposits burying older deposits

C= % slides which have reactivated, freshening older, subdued morphology, includes cases where more recent movement freshens a large enough portion of an older slide mass that it is missed during mapping

Implications of Temporal Distribution for Trigger Mechanisms

The corrected temporal distribution of landslides, if it approximates the actual distribution, may shed light on whether long-term climatic changes significantly influence the frequency of landsliding. Two opposing models can be proposed: 1) landslides occur more frequently during cool/wet climate cycles, contemporaneous with glacial advances, due to elevated groundwater levels, or 2) landslides occur rather uniformly through time, triggered by short-term climate events, individual intense storms, or earthquakes which occur randomly regardless of longer-term cycles. For the post-glacial period, the hypothetical temporal distribution of landslides produced by either the climate or uniform model can be compared to the corrected temporal distribution to look for similarities.

TABLE 3: CORRECTED TEMPORAL DISTRIBUTION

Age-Class	# Slides mapped	% Detection (from table 2)	Corrected # of slides	% of corrected # of slides
		Rockslides		
1	6	100	6	9
2	23	95	24.2	36
3	25	85	29.4	43
3+	6	75	8	12
Totals	60		67.6	100%
		Slump-Earth flows		
1	60	100	60	5
2	319	80	398.7	32
3	395.5[1]	50	790	63
Totals	774.5		1249.7	100%
		Debris flows		
1	42.5	99	42.9	8
2	104.5	50	209	39
3	28	10	280	53
Totals	175		531.9	100%
		Earth flows		
1	3	100	3	7
2	18	65	27.7	65
3	3	25	12	28
Totals	24		42.7	100%

[1]Numbers of slides assigned to an age-class range, e.g., 2-3, were divided by two and each half was assigned to a single age class, e.g., seven Age-Class 2-3 slides would be divided into 3.5 Age-Class 2 slides and 3.5 Age-Class 3 slides

Fig. 7. Histogram comparing the corrected landslide temporal distributions (four right columns) with various forcing mechanisms (four left columns). Ages, durations, and severities of Holocene climatic cycles are adapted from Miller and Birkeland (1974), Mahaney (1978) and Porter and others (1983).

Fig. 7 shows three hypothetical and four corrected landslide age distributions. In the climate model, the time span of age class 3 (5,000-14,000 yr BP) was dominated by the Altithermal Interval of warm, dry climate (5,000-8,000 yr BP) and by the warming trend responsible for the Pinedale deglaciation, interrupted only by the early Holocene glacial advance at roughly 10 ka. In contrast, age class 2 spans the Neoglacial period, composed of at least three different glacial advances. For these reasons the severity and extent of cool/wet climates is taken to be roughly twice as great in class 2 as in class 3, suggesting we should observe an increase in climate-triggered slides in class 2. In the uniform model, the number of landslides occurring in each age class is directly proportional to the time span of the class.

For rockslides, the corrected temporal distribution closely parallels the uniform distribution. This result was surprising because we expected a temporal concentration of rockslides immediately upon deglaciation and loss of valley wall support, followed by a lower rate of sliding. The temporal distribution suggests that rockslides have continued to occur rather uniformly with time, presumably in response to either continued downcutting of streams undermining dipping strata, earthquake shaking, random severe storms, or a combination of these causes. As an example, the famous Lower Gros Ventre, Wyoming rockslide of 1925 has been attributed to intense rainfall and a possible earthquake shock. Rockslides C-14 dated by Whitehouse and Griffiths (1983) in New Zealand also appear to be uniformly distributed in time, probably triggered by episodic earthquake shaking. Thus, it does not appear that the occurrence of rockslides is significantly affected by long-term climate cycles or the indirect erosional effects thereof.

Slump-flows (which comprise 76% of all landslides) display a temporal distribution very similar to that predicted by the uniform model, suggesting that they too are relatively unaffected by long-term climatic changes. It is possible that

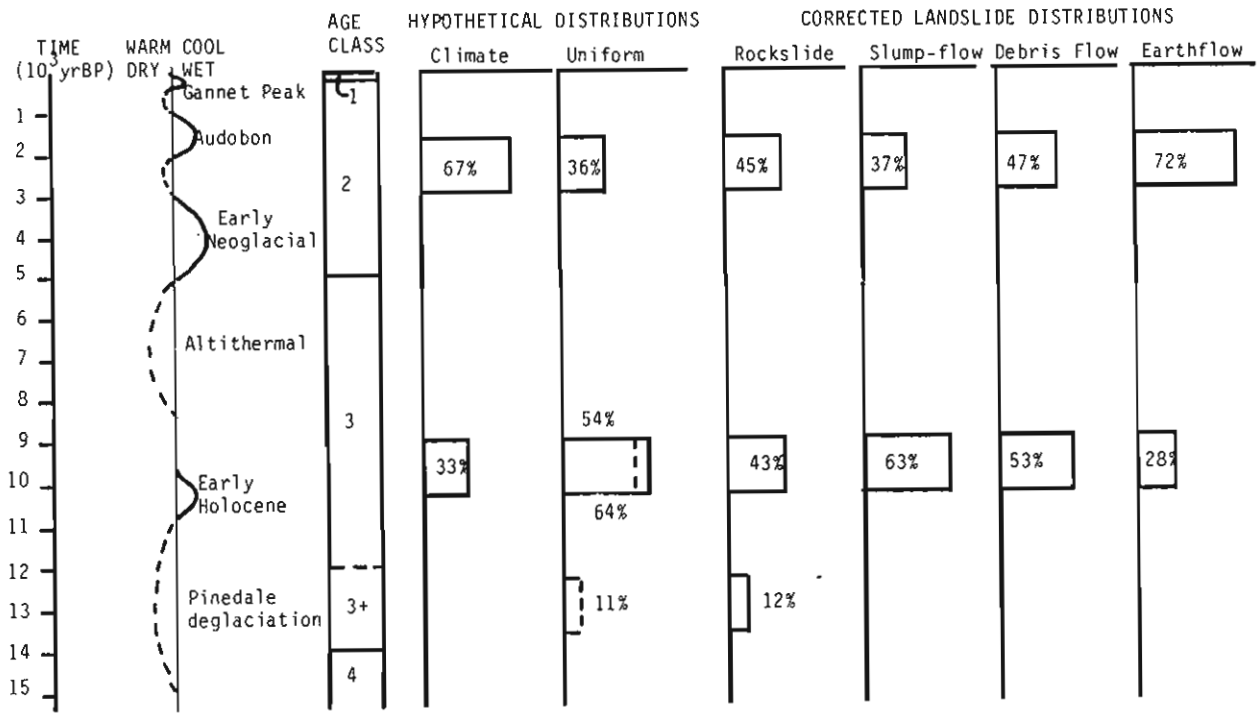

within age classes 2 and 3 there are temporal clusters of landslides which mimic individual stadial and interstadial periods, but such fine-scale differentiation is not possible without abundant absolute dates.

Debris flows exhibit a temporal distribution intermediate between that predicted by the climate and uniform models, suggesting that both long-term and short-term causes are important. Abundant historic debris flows in Utah in the 1930's were triggered by spring and summer rainstorms ("cloudbursts"), while those of 1983-84 were triggered by rapid melt of an above-average snowpack (Anderson et al 1984), both short-term causes. Longer-term controls on debris flows originating in colluvium-filled swales have been proposed by Reneau and others (1986). They hypothesize that swales are excavated to bedrock during wet cycles, slowly fill with colluvium during dry cycles, and are re-excavated by debris slides in the next wet cycle. If Salt River Range swales were filling during Altithermal time (class 3) and were then excavated in Neoglacial time (class 2), the long-term portion of the trigger mechanism could be accounted for.

Earthflows are relatively rare except in the Cretaceous section, and exhibit a temporal distribution most similar to the climate model, thus contrasting with all other slide types. Of all the slide types, earthflows contain the highest volume of water and the most impermeable material. It is therefore conceptually reasonable that long-term changes in groundwater level might affect earthflows more than other slides. Work by Jensen (1983) and Palmquist and others (1981) on the Upper Gros Ventre earthflow indicates that it moves periodically in response to both long-term and short-term climate variations. However, earthflows are also the most difficultto assign to morphologic age classes because of their unique morphology, and their tendency to continuously reactivate. Therefore, the apparent abundance of class 2 as opposed to class 3 earthflows may merely be an artifact of underestimating the extent of reactivation of older flows.

CONCLUSIONS

Landsliding in the Salt River Range, Wyoming, has occurred throughout Holocene time, strongly controlled by bedrock stratigraphy and structure. Of the 17 pre-Cretaceous stratigraphic units, 4 formations account for 46% of all landslides. Cretaceous rocks are so prone to sliding that an average of 73% of the outcrop area has been disturbed since the late Pleistocene.

Of the four major landslide types, only earthflows seem to have been strongly affected by small climatic shifts (epicycles of Crozier, 1986, p. 114) during the Holocene. The corrected temporal distribution of rockslides, slump-flows, and debris flows appears fairly uniform within the last roughly 14,000 yrs. A major difficulty in using landslide inventories from aerial photographs to reconstruct the chronology of landsliding is the unknown effect of erosion, burial, or reactivation on individual landslides.

ACKNOWLEDGEMENTS

This study received support from the U.S. Department of Agriculture, Forest Service, Bridger-Teton National Forest, and from the Office of Research, Utah State University, Logan, Utah.

REFERENCES

Anderson, L.R., Keaton, J.R., Saarinen, T.F. and Wells, W.G. II, 1984, The Utah Landslides, debris-flows, and floods of May and June, 1983: Commission on Engineering and Technical Systems, National Research Council, National Academy Press, 96 p.

Bailey, R.G., 1971, Landslide hazards related to landuse planning in Teton National Forest, northwest Wyoming: U.S. Department of Agriculture, Forest Service, Intermountain Region, 131 p.

Burke, R.M. and Birkeland, P.W., 1979, Re-evaluation of multiparameter relative dating techniques and their application to the glacial sequence along the eastern escarpment of the Sierra Nevada, California: Quaternary Research, v. 11, no. 1, p. 21-51.

Crozier, M.J., 1986, Landslides; causes, consequences, and environment: Croom Helm Ltd., 252 p.

Denton, G.H. and Porter, S.C., 1970, Neoglaciation: Scientific American, v. 222, no. 6, p. 101-110.

Jensen, J.M., 1983, The Upper Gros Ventre landslide of Wyoming: a dendrochronology of landslide events and the possible mechanics of failure: Geological Society of America, Abstracts with Programs, v. 15, no. 5, p. 387.

Mahaney, W.C., Halvorson, D.L., Piegat, James and Sanmugadas, K., 1984, Evaluation of dating methods used to assign ages in the Wind River and Teton Ranges, western Wyoming, in Mahaney, W.C., (ed.), Quaternary Dating Methods, p. 355-374, Elsevier.

McCalpin, James, 1984, Preliminary age classification of landslides for inventory mapping: Proceedings 21st Engineering Geology and Soils Engineering Symposium, University of Idaho, Moscow, Idaho, April 5-6, 1984, p. 99-120.

Palmquist, R.C., Cloud, T.A. and Jensen, J., 1981, Landslide history, middle reach of the Gros Ventre River Valley, Wyoming: National Geographic Society Final Report, grant no. 2134-80, 16 p.

Piety, L.A., 1987, Late Quaternary surface faulting on the Star Valley Fault, west-central Wyoming: Geological Society of America, Abstracts with Programs, v. 19, no. 5, p. 327.

Porter, S.C., 1980, Rapid deglaciation of alpine regions at the end of the last glaciation: Abstracts, 6th Biennial Meeting, American Quaternary Association, Orono, Maine, p. 157.

Porter, S.C., Pierce, K.L. and Hamilton, T.D., 1983, Late Wisconsin mountain glaciation in the western U.S., in Porter S.C. (ed.), Late Quaternary Environments of the United States, v. 1, The Late Pleistocene: University of Minnesota Press, Minneapolis, p. 71-111.

Reneau, S.L., Dietrich, W.E., Dorn, R.I., Berger, C.R. and Rubin, M., 1986, Geomorphic and paleoclimatic implications of latest Pleistocene radiocarbon dates from colluvium-mantled hollows, California: Geology, v. 14, no. 8, p. 655-658.

Rice, J.R. Jr., 1987, Spatial and temporal landslide distribution and hazard evaluation analyzed by photogeologic mapping and relative dating techniques, Salt River Range, Wyoming: M.S. Thesis, Utah State University, 129 p., map scale 1:48,000.

Romesburg, H.C. 1984, Cluster Analysis for Researchers: Lifetime Learning Publications, Belmont, California, 334 p.

Rubey, W.W., 1973, Geologic map of the Afton Quadrangle and part of the Big Piney Quadrangle, Lincoln and Sublette Counties, Wyoming: U.S. Geological Survey, Miscellaneous Geological Investigation Series, Map I-686, scale 1:62,500.

Varnes, D.J., 1978, Slope movement types and processes, in Schuster, R.L. and Krizek, R.J. (eds.), Landslides; analysis and control: Transportation Research Board, Special Report 176, p. 11-33.

Whitehouse, I.E. and Griffiths, G.A., 1983, Frequency and hazards of large rock avalanches in central and southern Alps, New Zealand: Geology, v. 11, no. 6, p. 331-334.

RELATIVE DATING PARAMETERS

Appendix A

1) Maximum pit depth. The maximum depth (mm) of weathering pits measured perpendicular to the stone surface.

2) Resistate inclusion height. The maximum surface relief (mm) of resistate inclusions measured perpendicular to stone surface.

3) Surface boulder frequency. The number of boulders with an estimated maximum dimension greater than 30 cm exposed at or on the surface within a 30 m by 6 m area on moraine crests.

4) Boulder burial factor. The product of the percentage of boulders with a maximum dimension greater than 30 cm which are partially buried, multiplied by the average volume percentage of burial of boulders (visual estimates).

5) Ridge crest width. The average horizontal width (m) of the surface zone at the top of a ridge which has an estimated surface slope of 5^{o} or less.

6) Maximum outer slope angle. Maximum measured slope (degrees) of the outer surface of sampled ridges (moraine or landslide pressure ridges in this study).

7) Maximum inner slope angle. Maximum measured slope (degrees) of the inner (proximal) surface of sampled ridges.

8) Soil profile development. The degree of subsurface weathering and horizonation on sampled deposits as determined from analysis of 60 cm deep soil pits.